Numerical Simulations of Fluorescence Resonance Energy Transfer in Diblock Copolymer Lamellae

Jian Yang and Mitchell A. Winnik*

Department of Chemistry, University of Toronto, 80 St. George Street, Toronto, Ontario, Canada M5S 3H6

Tadeusz Pakula†

Max-Planck-Institute für Polymerforschung, D-55021 Mainz, Postfach 3148, Germany

Received April 19, 2005; Revised Manuscript Received August 8, 2005

ABSTRACT: We describe numerical simulations of fluorescence resonance energy transfer (FRET) in symmetric diblock copolymer lamellae. The model systems were generated by Monte Carlo simulation at various finite temperatures, and virtual dyes (donors (D) and acceptors (A)) were introduced at the junction points of the block copolymer chains. We examined the effect of dye dipole orientation on energy transfer by selectively choosing the dipole orientations. The coupling effect between dipole orientation and D−A distance in the calculation of extent of energy transfer was found to be significant when donors and acceptors were confined to a thin interface at a low simulation temperature. We calculated the interface thickness of the simulated diblock copolymer lamellae based on the FRET data and the Helfand−Tagami mean field theory of polymer interfaces. FRET operates over short distances and is insensitive to the waviness of the interface.

Introduction

Symmetric diblock copolymers undergo microphase separation to form a spatially periodic lamellar morphology when the product of the Flory−Huggins interaction parameter (χ_{FH}) and the overall polymer chain length (N) is greater than 10.4.[1] Our research group has been interested in using fluorescence resonance energy transfer (FRET) measurements to study block copolymer interfaces.[2−5] These experiments involve pairs of diblock copolymers, one of which contains a fluorescence donor (e.g., phenanthrene (Phe)) and the other which contains an acceptor (e.g., anthracene (An)) at the junction of two blocks. Because the dyes are covalently bound to the junction, they are confined to the interface when the system is microphase separated. FRET is very sensitive to the distribution of distances between the donors and acceptors. By measuring the rate and extent of energy transfer from donors to acceptors, one can obtain information about the spatial distribution of the attached chromophores. In the context of theories of polymer interfaces, the width of the interface can be retrieved. To analyze the data generated in these kinds of experiments, our group has developed a model of FRET kinetics based on Zumhofen−Klafter−Blumen[6−8] concepts of energy transfer in restricted geometries.[9] We were able to use this approach to determine the thickness of the lamellar interface for several diblock copolymers, e.g., poly(isoprene-*b*-methyl methacrylate),[10,11] poly(styrene-*b*-methyl methacrylate),[12] and poly(styrene-*b*-butyl methacrylate).[13]

While the FRET kinetics employed in these studies have been thoroughly discussed in our previous reports,[10−12] this analysis depends on two assumptions. The first is that the orientation factor κ^2 for energy transfer between each pair of chromophores can be replaced with a preaveraged value $\langle|\kappa|\rangle^2$. To analyze experimental data for rigid films, we used the value $\langle|\kappa|\rangle^2 = 0.476$ appropriate for randomly distributed immobile chromophores in three dimensions. This approach assumes that there is no net orientation of the dyes attached to the junction when confined to the block copolymer interface. It also neglects any possible coupling between the donor−acceptor separation and their dipole orientation in determining the FRET rate for individual pairs of dyes. This type of coupling has been found to be important for the case of an ensemble of species consisting of a single donor and acceptor attached to a common flexible molecule; here the magnitude of the coupling decreased with increasing donor−acceptor separation.[14]

The second assumptions concerns the way the distribution of dyes in the interface is treated. In our experiments, we analyzed the distribution of rates of FRET in terms of a one-dimensional model, the Helfand−Tagami mean field theory,[15] which describes the distribution of the junctions along the z-axis, normal to the lamellar interface. More recently, others in our group have used a self-consistent theory[16] to obtain a more detailed description of the junction distribution profile along the z-direction. They then used these distributions to simulate actual experiments, in which the variable that they optimized in comparing experimental and simulated data was the width of the interface. These one-dimensional models are very effective and yield reasonable results for determination of the interface thickness for symmetric diblock copolymer lamella, but they do not take explicit account of FRET between donors and acceptors in the (x,y) plane of the interface.

While these assumptions cannot be tested directly by experiments, they can be examined numerically through mathematical simulations. Simulations allow one to take a broader approach to analyze the energy transfer process. Specifically within the context of FRET experiments, one can use Monte Carlo (MC) simulations to

* To whom correspondence should be addressed.

† Dr. Pakula passed away in June 2005. This paper is dedicated to his memory.

10.1021/ma0508303 CCC: $30.25
Published on Web 09/24/2005

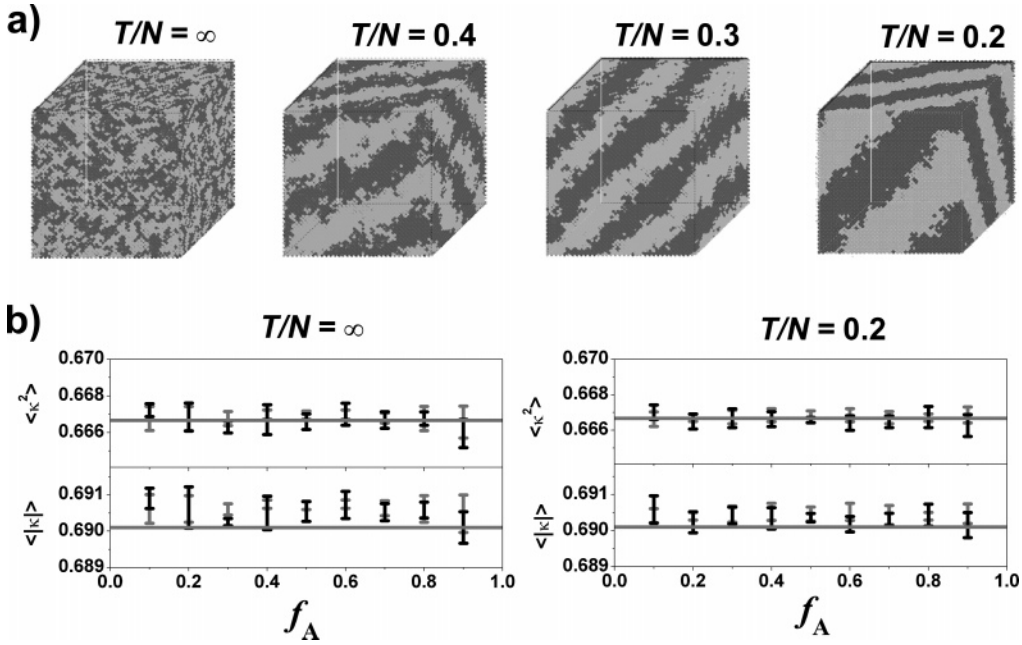

Figure 1. (a) Three-dimensional final morphologies for symmetric diblock copolymers (chain length = 70) in the 70 × 70 × 70 fcc lattice box at four different temperatures as indicated in the figure. Different blocks are identified using different colors and bonds are omitted. (b) Relationships between $\langle\kappa^2\rangle$ (two upper figures) or $\langle|\kappa|\rangle$ (two lower figures) and the fraction of acceptor (f_A) at $T/N = \infty$ and 0.2. The black error bars are the values for randomly choosing the coordinate directions as the dipole orientation. The gray error bars are those for using junction vectors as the dipole orientation. The solid lines in the upper figures are the dynamic averaged values for $\langle\kappa^2\rangle = {}^2/_3$ in the homogeneous system. The solid lines in the lower two figures are $\langle|\kappa|\rangle = 0.690$, obtained by Baumann and Fayer[25] for immobile dipoles in the three-dimensional static homogeneous state. Temperatures are indicated in the figures. R_0 was chosen as $10a$, where a is the lattice constant.

generate the lamellar morphology of a symmetric diblock copolymer under a certain defined set of conditions. By locating a virtual dye at the junction point of each diblock copolymer chain, one can examine energy transfer within the entire restricted geometry defined by the junction distribution across the interface, not only in the direction normal to the interface plane. One can use these simulated structures to evaluate the contribution of dipole orientation to FRET kinetics. One can also generate simulated donor fluorescence decay profiles from which one can examine the meaningfulness of the one-dimensional model for the junction distribution when it is applied to three-dimensional systems. These simulations also allow us to examine the effect of dipole orientation on energy transfer in the simulated diblock copolymer lamella, by selectively choosing the dipole orientations of the virtual dyes.

In a previous publication, we described MC simulations of diblock copolymer lamellae[17] for systems generated at simulation temperatures below the order−disorder transition temperature. From our analysis of the conformation and the orientation of the simulated diblock copolymer chains, we found that the polymer underwent microphase separation, as expected. The overall dimensions of the diblock copolymer chains were stretched, while the individual block chains remained Gaussian. The polymer chains had only a moderate tendency to orient themselves perpendicular to the lamellar interface plane. There was no significant correlation in the orientation of the chain backbone at the junction between the blocks. This result indicates that chain stretching does not have much influence on the dipole orientation of dyes attached at the junction of the diblock copolymer chains.

In this paper, we describe the results of numerical experiments based on these simulated diblock copolymer lamellae. We introduce the concept of a dye at the junction by assuming that a virtual dye exists at the junction point of each diblock copolymer chain. The loci of the donor and acceptor dyes were established in this way. As will be shown in next section, the efficiency of energy transfer and fluorescence intensity decay can be calculated on the basis of the loci and the dipole orientations of these virtual dyes. We can use these numerical experiments to test the assumptions described above. Since these are simulated structures, we were also able to test some strong and unrealistic assumptions about the dye orientation to obtain a broader understanding of the effect of dye dipole orientation on energy transfer. In this way, we can start to understand how the rate of energy transfer depends on the coupling between the dipole orientation and the D−A distance when donors and acceptors are confined within the small scale restricted geometry of the lamellar interface.

Construction of the Model FRET Systems. The model systems, simulated diblock copolymer lamellae, were generated by Monte Carlo simulation as described ref 17. The simulations were performed on a face-centered-cubic (fcc) lattice (coordination number $z = 12$) with bond length $\sqrt{2}a$ (a is the lattice constant) in a 70 × 70 × 70 dimension simulation box. Periodic boundary conditions were applied in all three dimensions in order to reduce boundary effects. The symmetric diblock copolymer chain had 70 monomeric units, and each block had 35 units. Four systems simulated at different simulation temperatures ($T/N = \infty$, 0.4, 0.3, 0.2) will be examined in this paper. These systems are shown in Figure 1a. The system forms well-defined lamellar structures when the simulation temperature is lower than the order−disorder transition temperature. At $T/N = \infty$, we obtained a homogeneous system. Only the

junction point, which is the midpoint of 35th and 36th beads, is considered as the location of the virtual dye. Thus, each polymer chain contains only one dye, and the number of dyes (donors + acceptors) is equal to the number of polymer chains in the lattice. The donors and acceptors are randomly chosen among the N_k virtual dyes in the lattice to give a predetermined fraction of acceptors

$$f_A = \frac{N_A}{N_k} = \frac{N_A}{N_A + N_D} \tag{1}$$

The Numerical FRET Method. Snyder and Freire[18−22] in the early 1980s were among the first to use Monte Carlo simulations to model FRET experiments in restricted geometries. They examined lattice models appropriate for FRET in lipid bilayer membranes and membrane proteins. Other groups, notably Blumen and Klafter[23,24] as well as Baumann and Fayer,[25] developed continuous models for examining FRET in restricted geometries. In a lattice system with an ensemble of donors and acceptors, the ensemble-averaged efficiency of energy transfer, Φ_{ET}, is given by the expression[18]

$$\Phi_{ET} = 1 - \frac{Q_{DA}}{Q_D}$$

$$\frac{Q_{DA}}{Q_D} = \frac{1}{N_D}\sum_{j=1}^{N_D}[1 + \sum_{k=1}^{N_A}\tau_D w(r_{jk})]^{-1}$$

$$w(r_{jk}) = \frac{3}{2}\frac{1}{\tau_D}\kappa_{jk}^2(\Omega)\left(\frac{R_0}{r_{jk}}\right)^6 \tag{2}$$

where Q_{DA}/Q_D is the ensemble-averaged ratio of the fluorescence quantum yield in the presence and the absence of acceptors. $w(r_{jk})$ is the rate of energy transfer between the jth donor and kth acceptor separated by a distance r_{jk}. τ_D is the unquenched donor lifetime. R_0 is the Förster radius, which is determined from the D−A spectral overlap integral along with the assumption that $\langle\kappa^2\rangle = {}^2/_3$. In this way, the magnitude of R_0 is independent of the orientation factor of individual D−A pairs.[26] The orientation factor, $\kappa^2(\Omega)$ (or $|\kappa(\Omega)|$), for individual D−A pairs can be written as

$$\kappa^2(\Omega) = \left[\vec{D}\cdot\vec{A} - \frac{3}{|r|^2}(\vec{D}\cdot\vec{r})(\vec{A}\cdot\vec{r})\right]^2$$

$$|\kappa(\Omega)| = |\vec{D}\cdot\vec{A} - \frac{3}{|r|^2}(\vec{D}\cdot\vec{r})(\vec{A}\cdot\vec{r})| \tag{3}$$

where $\vec{D}$ and $\vec{A}$ are the unit vectors of the dipole orientation of donor and acceptor, respectively. $\vec{r}$ is the distance vector connecting the D−A pair, and $|r|$ is the distance between D and A. For an ensemble of D−A pairs in the lattice, the average orientation factor can be calculated using

$$\langle\kappa^2\rangle = \frac{1}{N_p}\sum_{j\in\text{donor}}\sum_{k\in\text{acceptor}}\kappa_{jk}^2(\Omega)$$

$$\langle|\kappa|\rangle = \frac{1}{N_p}\sum_{j\in\text{donor}}\sum_{k\in\text{acceptor}}|\kappa_{jk}(\Omega)| \tag{4}$$

where N_p is the total number of D−A pairs in the lattice.

If one uses the preaveraged orientation factor, $\langle\kappa^2\rangle$ (or $\langle|\kappa|\rangle^2$), the relative quantum yield (eq 2) can be simplified to

$$\frac{Q_{DA}}{Q_D} = \frac{1}{N_D}\sum_{j=1}^{N_D}\left[1 + \frac{3}{2}\langle\kappa^2\rangle\sum_{k=1}^{N_A}\left(\frac{R_0}{r_{jk}}\right)^6\right]^{-1} \tag{5}$$

On the basis of eqs 2 or 5, one can calculate the relative quantum efficiency of energy transfer if the relative positions of donors and acceptors are known in the system.

If one assumes that the concentration of excited donors is sufficiently low, the normalized fluorescence intensity decay can be written as

$$\frac{I(t)}{I_0} = \exp\left(-\frac{t}{\tau_D}\right)\Psi(t) \tag{6}$$

where $\Psi(t)$ is the survival probability of an excited donor at time t. In a lattice with one excited donor surrounded by many acceptors, at a fixed acceptor concentration, Ψ can be considered as an ensemble average over all possible acceptor configurations in the lattice[23]

$$\Psi(p,t) = \prod_k[1 - p + pE_k(r_k,t)]$$

$$E_k(t) = \exp[-tw(r_k)] \tag{7}$$

where $w(r_k)$ is the rate of energy transfer between the donor and kth acceptor separated by a distance r_k. Here p is the probability that a site is occupied by an acceptor. For a particular acceptor configuration

$$\Psi(t) = \prod_k E_k(r_k,t) \tag{8}$$

Equation 8 always gives an exact exponential decay function. If a lattice system contains N_D donors and N_A acceptors, every donor has a different configuration of surrounding acceptors. As a consequence, the different excited donors have different survival probabilities. One can sum over all the probabilities and calculate the ensemble average of the survival probability of excited donors in the lattice[27]

$$\Psi(t) = \frac{1}{N_D}\sum_{j=1}^{N_D}(\prod_{k=1}^{N_A}E_{jk}(r_{jk},t)) \tag{9}$$

and the fluorescence intensity decay can be written as

$$I(t) = \frac{I_0}{N_D}\exp\left(-\frac{t}{\tau_D}\right)\sum_{j=1}^{N_D}\exp(-t\sum_{k=1}^{N_A}w(r_{jk})) \tag{10}$$

Equations 7 and 9 lead to the same results in the limit of a very large number (N) of lattice sites. For moderate N, the discrepancies will only be apparent for very long times.[23] Since our MC algorithm give the exact loci of the donors and acceptors in the lattice, it is not necessary to consider different acceptor configurations around each excited donor. One can average the survival probabilities for all excited donors using eq 9. Several configurations of donors and acceptors for each donor and acceptor concentrations will still be considered to

calculate the standard deviation of efficiency of energy transfer and fluorescence decay.

Results and Discussion

Orientation Factor. The preaveraged orientation factor can be calculated by eqs 3 and 4 based on the individual dipole orientations of the virtual dyes. We considered two cases for the dipole orientation: In the first case, the dipole orientation was chosen randomly to lie along any of the 12 coordinate directions to the closest-neighbor lattice sites. In the second case, the dipole orientation was directed along the junction vector, defined as a vector from the 35th bead (block A) to the 36th bead (block B) of the polymer chain. In this way we can test whether different dipole orientations can affect the value of the averaged orientation factor. In the calculations, we examined every donor in the model system and considered all of the acceptors around this donor within a sphere whose radius was $5R_0$. Here the Förster radius R_0 was chosen as $10a$. When the location of the acceptor in the sphere was outside of the simulation box, the periodic boundary conditions were applied. The orientation factor was averaged by summing over all the donors in the simulation box. Figure 1b shows the calculated preaveraged orientation factor at two different simulation temperatures ($T/N = \infty$ and 0.2) as a function of acceptor fraction in the system. From the figure, one can see that although $\langle\kappa^2\rangle$ was calculated for immobile transition dipoles, all of the calculated values are very close to the value ($^2/_3$) corresponding to the dynamic average for a homogeneous system. The value does not change even at low temperature ($T/N = 0.2$), where the interface is narrow and the junction points are much closer to each other than at higher temperatures.

Baumann and Fayer[25] used a numerical method to calculate excitation transfer in three-dimensional disordered systems. For a static three-dimensional homogeneous system, they found that the preaveraged orientation factor $\langle|\kappa|\rangle$, not $\langle\kappa^2\rangle$, can be retrieved and the value was found to be 0.6901. The static average value for randomly distributed dyes, 0.476, can be then calculated by squaring $\langle|\kappa|\rangle$. We calculated $\langle|\kappa|\rangle$ on the basis of the simulated systems as shown in the lower two plots in Figure 1b. The values are very close to the value calculated by Baumann and Fayer. The slight deviation between our values and Baumann and Fayer's value possibly results from drawbacks of the lattice model. It seems that the statistically averaged orientation factor, $\langle|\kappa|\rangle$ or $\langle\kappa^2\rangle$, is unchanged no matter how far the dipoles are separated in the three-dimensional system.

Efficiency of Energy Transfer. Both eqs 2 and 5 can be used to calculate Φ_{ET} based on the loci of junction points (dyes), depending on how one chooses the orientation factor. We start with the homogeneous model system ($T/N = \infty$) to test the feasibility of the methodology to calculate Φ_{ET} numerically. Here we chose four different ways to consider the dipole orientation: preaveraged values of $\langle\kappa^2\rangle = {}^2/_3$ and $\langle|\kappa|\rangle^2 = 0.476$; the junction vector as the dipole orientation and the random selection of the dipole orientation within the 12 closest coordinate directions. In first two cases, we used the preaveraged values and eq 5 to calculate Φ_{ET}. In the last two cases, instead of preaveraging the orientation factor, we calculated individual orientation factors for each D−A pair by considering the dipole orientations

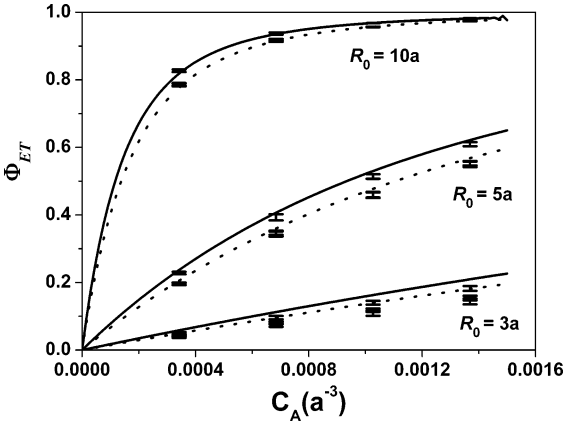

Figure 2. Efficiency of energy transfer (Φ_{ET}) calculated using eqs 2 and 5 in homogeneous 3D systems with different R_0. The values of R_0 are indicated in the figure. There are two major parts for each R_0: the upper part presents the values of Φ_{ET} obtained by assuming $\langle\kappa^2\rangle = {}^2/_3$; the lower part consists of three overlapped Φ_{ET} values, which were obtained by selecting the junction vector as the orientation dipole; by randomly selecting the dipole orientation; and by using $\langle|\kappa|\rangle^2 = 0.476$. The solid and dotted lines are the theoretical curves obtained by eq 11 for $\langle\kappa^2\rangle = {}^2/_3$ and $\langle|\kappa|\rangle^2 = 0.476$, respectively. C_A is the acceptor concentration in the simulated system, calculated from $C_A = N_A/V$, where V is the volume of the simulation box.

of the donor and the acceptor (eq 3) and used eq 2 to calculate Φ_{ET}. Three different R_0 values were chosen as well. As shown in Figure 2, for each R_0 and a certain acceptor concentration, the Φ_{ET} values were calculated by assuming $\langle|\kappa|\rangle^2 = 0.476$; the junction vector as the dipole orientation and a random selection of dipole orientation are in good agreement with each other. All three values are smaller than the Φ_{ET} value calculated assuming that $\langle\kappa^2\rangle = {}^2/_3$. The results provide proof that $\langle|\kappa|\rangle^2$, rather than $\langle\kappa^2\rangle$, is the better preaveraged value for the orientation factor for FRET in homogeneous three-dimensional systems.[28]

As a comparison, we also calculated the efficiency of energy transfer (Φ_{ET}) in the homogeneous three-dimensional systems using the Förster equations[29]

$$\Phi_{ET} = \sqrt{\pi}\gamma \exp(\gamma^2)[1 - \mathrm{erf}(\gamma)]$$

$$\gamma = C_A \frac{2}{3}\pi^{3/2} N_0 \sqrt{\frac{3}{2}\langle|\kappa|\rangle^2} R_0^3$$

$$\mathrm{erf}(\gamma) = \frac{2}{\pi}\int_0^\gamma \exp(-x^2)\,dx \qquad (11)$$

where C_A is the concentration of acceptor in the system and N_0 is the Avogadro constant. We show the calculation results for different R_0 values in Figure 2 by taking two preaveraged orientation factors: $\langle|\kappa|\rangle^2 = 0.476$ (dotted lines) and $\langle\kappa^2\rangle = {}^2/_3$ (solid lines). For each R_0, the results calculated by both eq 5 and eq 11, employing a preaveraged orientation factor ($\langle|\kappa|\rangle^2 = 0.476$ or $\langle\kappa^2\rangle = {}^2/_3$), are in good agreement with each other. The largest discrepancy was found for the smallest R_0 value ($R_0 = 3a$). When R_0 is small, on the order of few lattice lengths, the discrete nature of the lattice model limits the number of sites that can be included in a FRET calculation.

We performed similar calculations for the model system at $T/N = 0.2$ and show the results in Figure 3. The data presented refer to $R_0 = 5a$. We employed the same four different cases of dipole orientation as for the

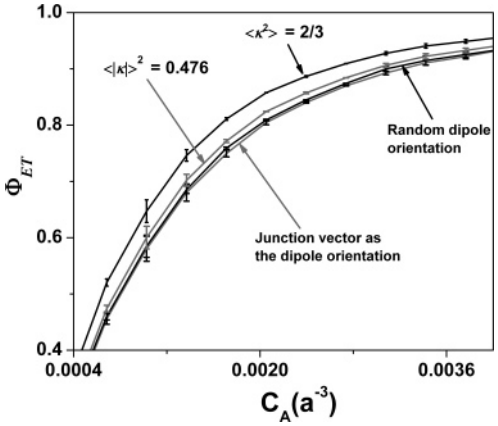

Figure 3. Efficiency of energy transfer (Φ_{ET}) calculated using eqs 2 and 5 for the simulated diblock copolymer lamella at $T/N = 0.2$ and $R_0 = 5a$. The selections of dipole orientation (four cases) are indicated in the figure.

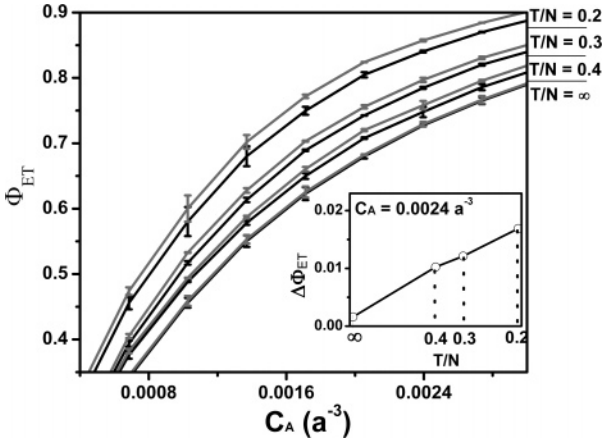

Figure 4. Efficiency of energy transfer (Φ_{ET}) vs acceptor concentration at different simulation temperatures (T/N) indicated in the figure. R_0 was fixed at $5a$. There are two lines with error bars for each temperature, representing the two cases of different selections of dipole orientation: the gray line is for Φ_{ET} values calculated by assuming the preaveraged orientation factor, $\langle|\kappa|\rangle^2 = 0.476$ (eq 5); the black line is for Φ_{ET} values calculated considering individual orientation factors for each D−A pair by choosing the junction vectors as the dipole orientation (eq 2). Inset: the difference in Φ_{ET} values ($\Delta\Phi_{ET}$) calculated for the two dipole orientation choices at a fixed acceptor concentration ($C_A = 0.0024a^{-3}$).

calculations of the homogeneous system ($T/N = \infty$). As shown in Figure 3, for each acceptor concentration, Φ_{ET} values calculated by assuming $\langle\kappa^2\rangle = {}^2/_3$ are higher than those obtained using the other three treatments of the orientation factor. Unlike the case of $T/N = \infty$, differences appear for the model system at $T/N = 0.2$, among these three cases of dipole orientation. For example, at $T/N = 0.2$, the preaveraged value of the orientation factor, $\langle|\kappa|\rangle^2 = 0.476$, gives a slightly higher value of Φ_{ET} than for the cases where Φ_{ET} was calculated without preaveraging the orientation factor. For this situation, Φ_{ET} values were essentially identical if the dipole orientation was random or directed along the backbone vector. At lower temperatures, the interface between two blocks becomes sharper. Since the virtual dyes are located at the junction of two blocks, the dyes (donors and acceptors) move closer and are confined to a narrow restricted geometry when the temperature decreases.

Our results show that the coupling effect between dipole orientation and D−A distance on the extent of energy transfer becomes more apparent when the D and the A dyes move closer, even though the value of $\langle|\kappa|\rangle^2$ remains unchanged. Although this effect is very small, our results show that at the highest level of precision one cannot simply preaverage the orientation factor from all of the individual orientation factors for each D−A pair in systems in which the donor−acceptor separation is small. This is the conclusion reached by Wu and Brand,[14] who used numerical methods to analyze FRET kinetics for molecules containing a single donor−acceptor pair, where the objective was to determine the separation distance between the dyes (the "spectroscopic ruler") by a FRET experiment. In their system, for dyes at short separations, it was not possible to employ a preaveraged orientation parameter because the magnitude of κ^2 and distance were coupled for each dye pair in a way that varied with dye separation distance.

To better understand the coupling effect of dipole orientation and D−A distance on the magnitude of Φ_{ET}, we carried out further calculations at the simulation temperatures of $T/N = 0.3$ and 0.4. For these calculations, R_0 was also fixed at $5a$. For clarity here, we chose only two dipole orientation cases in the calculation of Φ_{ET}. As shown in Figure 4, there are two lines with error bars for each simulation temperature: the gray line represents the values of Φ_{ET} calculated using the preaveraged value ($\langle|\kappa|\rangle^2 = 0.476$), and the black line represents the values of Φ_{ET} calculated using the junction vector as the dipole orientation to calculate the individual orientation factor for each D−A pair. As expected, Φ_{ET} increases with the decrease of temperature due to the narrowing of the interface and the closer approach of donors and acceptors. More interestingly, at a fixed acceptor concentration, the difference in Φ_{ET} values between those two dipole orientation cases (the two lines at each temperature) becomes larger when the simulation temperature decreases. An example of the temperature dependence of this difference for $C_A = 0.0024a^{-3}$ is shown in the inset of Figure 4. This result indicates that the coupling effect of dipole orientation and D−A distance becomes more pronounced when the donors and acceptors are confined to a narrower interface.

In our previous report,[11] we showed that FRET experiments on real diblock copolymer lamella were not sensitive to the position of attachment of the dyes at the junction of diblock copolymer chains. We concluded that a preaveraged orientation factor could be used to analyze the data from these FRET experiments. Indeed, it would be very difficult to analyze these data without making assumptions involving a preaveraged orientation factor. From the results described in this paper, we learn that if one has to use a preaveraged orientation factor to calculate Φ_{ET} for a system in which donors and acceptors are confined to a narrow geometry, a value of $\langle|\kappa|\rangle^2$ somewhat smaller than 0.476 is more appropriate to represent the orientation factor in the system. For example, for the simulated diblock copolymer lamella at $T/N = 0.2$, with the dyes located at the interface, the optimum preaveraged orientation factor was found to be $\langle|\kappa|\rangle^2 = 0.43 \pm 0.02$, which is an intermediate value between those appropriate for 3D ($\langle|\kappa|\rangle^2 = 0.476$) and 2D ($\langle|\kappa|^{2/3}\rangle^3$) = 0.405) homogeneous dipole distributions.[25]

Fluorescence Decays at Different Simulation Temperatures. Fluorescence intensity decay profiles can be calculated using eq 10 for the simulated diblock copolymer lamellae. Unquenched donor decays are

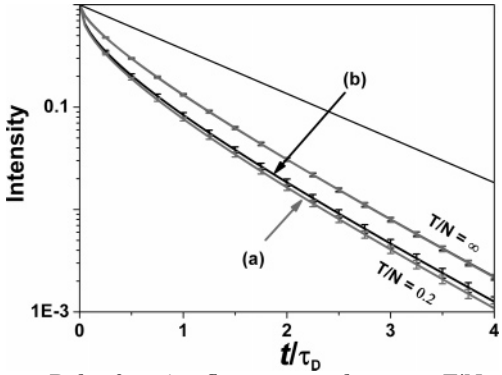

Figure 5. Delta function fluorescence decays at $T/N = \infty$ and $T/N = 0.2$ for $f_A = 0.2$. There are two decay curves for each temperature: the gray lines (a) with error bars are the decays calculated assuming $\langle|\kappa|\rangle^2 = 0.476$. The black lines (b) are the decays calculated by considering individual orientation factors for each D−A pair, assuming the junction vector as the dipole orientation. The temperatures are indicated in the figure. The upper straight line is the single-exponential decay in the absence of acceptors.

predicted to be exponential. In the presence of acceptor, the time-resolved fluorescence intensity of donor will deviate from a single-exponential decay law. In this section, we describe calculations of the donor fluorescence intensity decay profiles for the simulated diblock copolymer lamellae at different temperatures and at different f_A values. In all of these calculations, R_0 was fixed at $5a$, and the junction vector was chosen as the dipole orientation.

In the Supporting Information, we present fluorescence intensity decays for different acceptor fractions at $T/N = 0.3$ (Figure S1). The deviation of the decay from an exponential profile increases with the acceptor fraction. The systems with higher acceptor fraction gave faster decays at early times after instantaneous excitation. We also present the donor fluorescence decays for different temperatures at a fixed acceptor fraction ($f_A = 0.2$, Figure S2) in the Supporting Information. The fluorescence intensity of the system at lower simulation temperature decays faster than that of the system at higher temperature due to the higher local concentration of donors and acceptor when the interface narrows.

To test the effect of dipole orientation on the simulated fluorescence decay profiles, we chose two cases for the orientation factor. In the first calculation, we considered the individual orientation factors for each D−A pair by assuming the junction vector as the dipole orientation; in the second, we used the preaveraged orientation factor, $\langle|\kappa|\rangle^2 = 0.476$. Figure 5 shows the fluorescence decays calculated with these two dipole orientations at two simulation temperatures ($T/N = \infty$ and 0.2) at a fixed acceptor fraction ($f_A = 0.2$). Good overlap for the decays calculated from the homogeneous system ($T/N = \infty$) can be clearly observed, while at the lowest temperature ($T/N = 0.2$), the preaveraged orientation factor 0.476 gives a somewhat faster decay than the profile calculated by considering individual dipole orientations. This is consistent with the results we obtained in the previous section. In narrow confined geometries, with small donor−acceptor separations, the preaveraged orientation factor 0.476 gives a slightly larger extent of energy transfer due to the coupling effect of the dipole orientation and the D−A distance.

Generation of Simulated Experimental Decay Profiles and Determination of Interface Thickness. In our previous publications,[10−12] we employed the Helfand−Tagami theory of diblock copolymer interfaces in conjunction with Yekta's model of FRET kinetics[9] to calculate the thickness of the interface from experimental data on PI−PMMA diblock copolymer lamella. This methodology considers a one-dimensional distribution of dyes in a direction normal to the interface. While this model is convenient for data analysis, it has the drawback of ignoring FRET events occurring within the plane of the interface. The lamellae obtained by MC simulation allow us to examine energy transfer within the entire junction distribution across the block copolymer interface. This provides an opportunity to examine the validity of the one-dimensional model.

To test these ideas, we generated simulated experimental fluorescence decay profiles by convoluting the delta-function fluorescence decays, calculated in the previous section, with an actual experimental instrument response function (see Supporting Information for details). Each of the simulated experimental fluorescence decay profiles was then fitted by the theoretical decay calculated by our FRET methodology in terms of a one-dimensional (1D) junction distribution across the interface, following the procedures described refs 10 and 11. In this way, the interface thickness can be obtained from the decay curve fitting. Since FRET is only effective within a few R_0, we anticipate that this experiment is insensitive to waviness in the interface plane. We could evaluate this effect by comparing the optimized 1D interface thickness to the value determined from the simulations,[30] which contains the contribution of the waviness. In addition, the goodness of fitting results would indicate the validity of using the 1D model for data analysis in the three-dimensional system.

We generated simulated experimental decays corresponding to three different simulation temperatures ($T/N = 0.2$, 0.3, 0.4) and three different acceptor fractions ($f_A = 0.1$, 0.2, 0.3). All of the decays were fitted as described in the Supporting Information. Figure 6 shows examples of the fits for $T/N = 0.3$. All of the fitting results at different values of T/N and f_A are listed in Table 1. From the χ^2 values, one can see that the goodness of fit becomes worse with the increase of acceptor fraction. When $f_A = 0.3$, the fitting is unacceptable. The quality of the fit also depends on the simulation temperature. Data obtained for higher simulation temperatures gave better fits of the simulated data to the model. The dependence of the fit on simulation temperature and acceptor fraction originates from the increase of local concentration of acceptors surrounding each excited donor. With the decrease of simulation temperature, the extent of microphase separation becomes enhanced, and the interface narrows. As a consequence, the dyes at the junction of the two blocks in a polymer chain become confined in a more restricted geometry, and the local concentration of acceptors around donors increases. These results indicate that the one-dimensional model is only applicable at low acceptor fraction and simulation temperature characterized by lower local acceptor concentrations around the excited donors.

Values of the thickness (δ) of the simulated diblock copolymer lamella interface retrieved from the decay curve fitting are shown in Table 1. For each simulation temperature, we obtained a similar interface thickness value at $f_A = 0.1$ and 0.2. For $f_A = 0.3$, the quality of the fit was poor, and the "best fit" thickness value of the interface thickness was smaller.

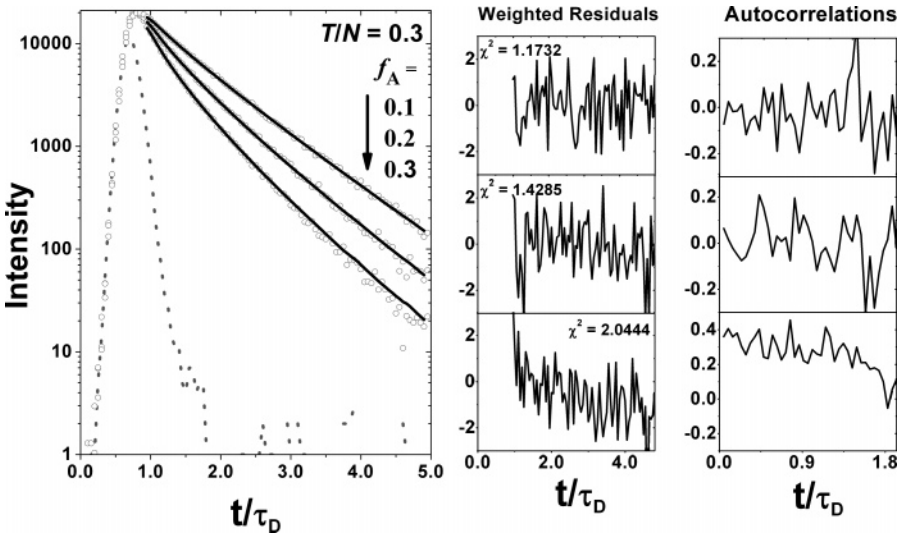

Figure 6. Fitting of simulated experimental fluorescence decays (open circles in the left figure) at three acceptor fractions (indicated in the figure) from the simulated diblock copolymer lamella at $T/N = 0.3$. τ_D is the unquenched donor lifetime in the absence of acceptor. The dotted line is an experimental instrument response function. The time scale of the instrument response function was normalized to $0.05t/\tau_D$ so that the experimental and simulated data had the same dimensionless time scale. The solid lines in the left figure are the best fits with the optimized interface thickness. Weighted residuals, autocorrelations, and χ^2 values[26] of the nonlinear least-squares fitting for each decay are shown on the right side of the figure.

Table 1. Fitting Results for Simulated Experimental Decays, Using the Helfand−Tagami Mean Field Theory and Yekta's FRET Kinetics

T/N	0.2	0.2	0.2	0.3	0.3	0.3	0.4	0.4	0.4
f_A	0.1	0.2	0.3	0.1	0.2	0.3	0.1	0.2	0.3
$\chi^{2\,a}$	0.935	2.251	4.303	1.172	1.429	2.044	1.289	1.522	1.708
δ	1.3a^b	1.3a	1.1a	2.0a	2.1a	1.7a	4.3a	4.2a	3.8a

[a] Nonlinear least-squares fit. [b] a is the lattice constant in the MC simulation.

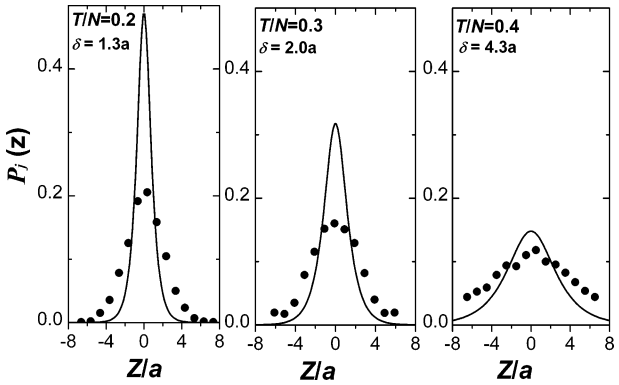

Figure 7. Junction distributions ($P_j(z)$) across the interface ($z = 0$) for the three simulation temperatures indicated in the figures. All distributions are normalized by the area of the peak. Filled points: data from the MC simulations. The distributions were obtained by three-dimensional rotation of the simulation box to align the interface perpendicular to the z-axis (see Figure 6 and its context in ref 17 for details). Solid lines: junction distributions calculated by Helfand−Tagami theory to fit the interface thickness (at $f_A = 0.1$, indicated in each figure) retrieved from fluorescence decay curve fitting.

To proceed more deeply into the analysis, we compare in Figure 7 the shapes of the interfaces inferred from the analysis of the simulated fluorescence decay profiles with the junction distribution obtained at each temperature from the MC simulation.[17,30] The junction distribution (filled points) obtained from the MC simulation includes two contributions: the "true" junction distribution across a flat interface plane and a contribution due to waviness of the interface. This waviness is known to contribute to experimental values of the interface thickness δ obtained by scattering and neutron reflectivity experiments. These experiments operate over a large range of length scales where this waviness would be expected to be prominent. The FRET experiment operates over such a short length scale (at most, a few R_0) that this waviness would not make a significant contribution to the value of δ calculated from the FRET data.

In Figure 7, we see that the width of the junction distribution calculated from the MC structures is significantly wider than the interface thickness obtained from the analysis of the simulated decay curves. The junction distribution represents a projection of the junction loci on the z axis. The shape of this distribution contains a contribution of the waviness of the lamellar structure within each simulation box. The "experimental" interface profiles (Helfand−Tagami junction profiles that match the best-fit δ values) are significantly narrower. These profiles reflect the fact that the characteristic length scale of the FRET experiment is much smaller than the width of the simulation box. These results emphasize the validity of the conclusion that FRET experiments on junction-labeled block copolymers show relatively little, if any, sensitivity to the waviness of the interface.

Summary

In this report, we described simulated FRET experiments based on block copolymer chain ensembles generated at various temperatures by Monte Carlo simulation. Virtual dyes (donors and acceptors) were introduced at the junction points of the chains. To calculate average orientation factors, we chose two different cases for the dipole orientation of the virtual dyes, and the average orientation factor, $\langle|\kappa|\rangle$, was calculated at different

simulation temperatures by summing over individual orientation factors for each D−A pair. The value obtained was independent of simulation temperature and was close to that (0.690) characteristic of a homogeneous three-dimensional distribution of immobile dyes. From the results of efficiency of energy transfer (Φ_{ET}) calculations and simulated fluorescence decay profiles, we found that this preaveraged orientation factor can well represent the dipole orientations in the simulated system at a high simulation temperature ($T/N = \infty$) corresponding to isotropic dye distribution. But at low simulation temperatures, this value of $\langle|\kappa|\rangle$ led to higher extents of energy transfer than in the case where the individual orientation factors for each D−A pair were summed separately. The differences were relatively small and varied with the simulation temperature as shown in the inset of Figure 4.

The decrease of the simulation temperature leads to narrowing of the interface and closer approach of the donors and acceptors. Under these circumstances, using a preaveraged orientation factor appropriate for homogeneous systems introduces errors in the calculation of donor decay profiles and FRET quantum yields. In narrowly confined geometries, the coupling effect of dipole orientation and D−A distance on energy transfer becomes pronounced due to the close proximity of donors and acceptors. In principle, it would be best if one could analyze data by considering the coupling of the orientation factor and the donor−acceptor distance. Since it is impossible to measure the orientation factor for each D−A pair experimentally, one has to choose a preaveraged orientation factor value to simplify the calculation of energy transfer. The error created is relatively small and can be rectified by using a slightly smaller value of $\langle|\kappa|\rangle^2$ than 0.476. We estimated, from Φ_{ET} values, that a smaller preaveraged orientation factor ($\langle|\kappa|\rangle^2 = 0.43 \pm 0.02$) would properly reproduce the extent of FRET in the simulated diblock copolymer lamella at $T/N = 0.2$ (with $R_0 = 5a$). Although this value cannot be used extensively in the calculation of energy transfer in other systems, we do suggest that one should use a preaveraged value for the orientation factor slightly smaller than $\langle|\kappa|\rangle^2 = 0.476$ when one wants to calculate energy transfer in the confined geometries, in which one of the confining dimensions is less than $2R_0$ in length.

More recent results from our laboratory have shown that the magnitude of the preaveraged orientation parameter can be estimated through simulations of planar-slab, cylindrical-shell, and spherical-shell geometries.[31] For a planar-slab geometry with a thickness equal to R_0, FRET experiments can be fitted effectively using $<|\kappa|>^2 = 0.42$.

In the final section of this paper, we described numerical experiments in which we generated the simulated experimental fluorescence decay profiles by convoluting delta-function decay profiles with an actual experimental instrument response function. The simulated experimental decays allowed us to test our previous FRET data analysis methodology for determining the interface thickness in diblock copolymer lamellae. Our results show that the methodology gives reasonable results, judged from goodness of decay fitting, at low acceptor fractions and relative broad interfaces, where the local concentration of acceptor around the excited donors are sufficiently small. At higher acceptor concentrations (i.e., $f_A > 0.3$ and low simulation temperatures) obvious deviations of the fit from the data were found. The junction distribution profile of diblock copolymer chain retrieved by these data analysis methodology is much narrower than junction distribution obtained in the MC simulations. This narrower junction distribution originates from the fact that the FRET experiment is not very sensitive to the waviness of the interface separating the two polymer lamella because of the short-distance nature of the FRET interaction. On the other hand, the junction distribution inferred from the MC calculation is obtained by projection the loci of the junction points onto a plane perpendicular to the interface. This distribution contains the full contribution of the waviness of the interface across the simulation box.

Because preaveraging the orientation factor even for relative narrow interfaces introduces only small errors in the analysis of FRET data, and because the FRET experiment is so insensitive to waviness of the lamellar interface, FRET experiments appear to represent a robust experimental technique to study block copolymer interfaces.

Acknowledgment. The authors thank NSERC Canada and the ORDCF program of the Province of Ontario for their support of this research.

Supporting Information Available: Plots of calculated delta function fluorescence decays at different acceptor fractions (at $T/N = 0.3$) and at different simulation temperatures (at $f_A = 0.2$), together with a detailed description of the method of generation of simulated experimental donor fluorescence decays and the FRET kinetics used for interface thickness determination for diblock copolymer lamella. This material is available free of charge via the Internet at http://pubs.acs.org.

References and Notes

(1) Bates, F.; Fredrickson, G. H. *Annu. Rev. Phys. Chem.* **1990**, *41*, 525.
(2) Ni, S.; Zhang, P.; Wang, Y.; Winnik, M. A. *Macromolecules* **1994**, *27*, 5742.
(3) Tcherkasskaya, O.; Ni, S.; Winnik, M. A *Macromolecules* **1996**, *29*, 610.
(4) Tcherkasskaya, O.; Ni, S.; Winnik, M. A *Macromolecules* **1996**, *29*, 4241.
(5) Tcherkasskaya, O.; Spiro, J. G.; Ni, S.; Winnik, M. A *J. Phys. Chem.* **1996**, *100*, 7114.
(6) Klafter, J.; Blumen, A. *J. Chem. Phys.* **1984**, *80*, 874.
(7) Klafter, J.; Drake, J. M. *Molecular Dynamics in Restricted Geometries*; Wiley: New York, 1989.
(8) Drake, J. M.; Klafter, J.; Levitz, P. *Science* **1991**, *251*, 1574.
(9) Yekta, A.; Duhamel, J.; Winnik. M. A. *Chem. Phys. Lett.* **1995**, *235*, 119.
(10) Yang, J.; Lu J.; Rharbi, Y.; Cao L.; Winnik, M. A.; Zhang, Y.; Weisner, U. *Macromolecules* **2003**, *36*, 4485.
(11) Yang, J.; Roller, R. S.; Winnik, M. A.; Zhang, Y.; Pakula, T. *Macromolecules* **2005**, *38*, 1256.
(12) Rharbi, Y.; Winnik, W. A. *Macromolecules* **2001**, *34*, 5238.
(13) Spiro, J.; Yang, J.; Zhang, J.; Winnik, M. A.; Rharbi, Y.; Vavasour, J.; Whitmore, M. S.; Jerome, R., manuscript in preparation.
(14) Wu, P.; Brand, L. *Biochemistry* **1992**, *31*, 7939.
(15) Helfand, E.; Tagami, Y. *J. Chem. Phys.* **1972**, *56*, 3592. Helfand, E. *Macromolecules* **1975**, *8*, 552. Helfand, E.; Wasserman, Z. R. *Macromolecules* **1980**, *13*, 994.
(16) Matsen, M. W.; Schick, M. *Phys. Rev. Lett.* **1994**, *72*, 2660.
(17) Yang, J.; Winnik, M. A.; Pakula, T. *Macromol. Theory Simul.* **2005**, *14*, 9.
(18) Snyder, B.; Freire, E. *Biophys. J.* **1982**, *40*, 137.
(19) Freire, E.; Snyder, B. *Proc. Natl. Acad. Sci. U.S.A.* **1980**, *77*, 4055.
(20) Freire, E.; Snyder, B. *Biochemistry* **1980**, *19*, 88.
(21) Freire, E.; Snyder, B. *Biochim. Biophys. Acta* **1979**, *600*, 643.
(22) Freire, E.; Snyder, B. *Biophys. J.* **1982**, *37*, 617.
(23) Blumen, A.; Manz, J. *J. Chem. Phys.* **1979**, *71*, 4694.
(24) Blumen, A.; Klafter, J. *J. Chem. Phys.* **1986**, *84*, 1397.
(25) Baumann, J.; Fayer, M. D. *J. Chem. Phys.* **1986**, *85*, 4087.

(26) Lakowicz, J. R., Ed. *Principles of Fluorescence Spectroscopy*; Plenum Press: New York, 1999.
(27) Wolber, P. K.; Hudson, B. *Biophys. J.* **1979**, *28*, 197.
(28) Dale, R. E.; Eisinger, J.; Blumberg, W. E. *Biophys. J.* **1979**, *26*, 161.
(29) Bennett, R. G. *J. Chem. Phys.* **1964**, *41*, 3037.
(30) The interface thickness (junction point distribution) can be obtained directly from the projection of junction loci in the simulated systems onto the plane perpendicular to the interface (cf. Figure 6 in ref 17).
(31) Yang, J.; Winnik, M. A. *J. Phys. Chem. B*, in press.

MA0508303